Physics and Imaging in Radiation Oncology 20 (2021) 82–87

Contents lists available at ScienceDirect

Physics and Imaging in Radiation Oncology

journal homepage: www.sciencedirect.com/journal/physics-and-imaging-in-radiation-oncology

Comparison of Library of Plans with two daily adaptive strategies for whole bladder radiotherapy

Duncan den Boer [a,*], Mariska D. den Hartogh [a,1], Alexis N.T.J. Kotte [a], Jochem R. N. van der Voort van Zyp [a], Juus L. Noteboom [a], Gijsbert H. Bol [a], Thomas Willigenburg [a], Anita M. Werensteijn-Honingh [a], Ina M. Jürgenliemk-Schulz [a], Astrid L.H.M.W. van Lier [a], Petra S. Kroon [a]

[a] Department of Radiotherapy, University Medical Center Utrecht, Heidelberglaan 100, 3584 CX Utrecht, the Netherlands

ARTICLE INFO

Keywords:
Bladder cancer
MR-guided radiotherapy
Daily online adaptive radiotherapy
Library of Plans

ABSTRACT

Background and purpose: Whole bladder radiotherapy is challenging due to inter- and intrafraction size and shape changes. To account for these changes, currently a Library of Plans (LoP) technique is often applied, but daily adaptive radiotherapy is also increasingly becoming available. The aim of this study was to compare LoP with two magnetic resonance imaging guided radiotherapy (MRgRT) strategies by comparing target coverage and volume of healthy tissue inside the planning target volume (PTV) for whole bladder treatments.

Methods and materials: Data from 25 MRgRT lymph node oligometastases treatments (125 fractions) were used, with three MRI scans acquired at each fraction at 0, 15 and 30 min. Bladders were delineated and used to evaluate three strategies: 1) LoP with two plans for a 15 min fraction, 2) $MRgRT_{15min}$ for a 15 min fraction and 3) $MRgRT_{30min}$ for a 30 min fraction. The volumes of healthy tissue inside and bladder outside the PTV were analyzed on the simulated post-treatment images.

Results: $MRgRT_{30min}$ had 120% and 121% more healthy tissue inside the PTV than LoP and $MRgRT_{15min}$. For LoP slightly more target outside the PTV was found than for $MRgRT_{30min}$ and $MRgRT_{15min}$, with median 0% (range 0–23%) compared to 0% (0–20%) and 0% (0–10%), respectively.

Conclusions: Taking into account both target coverage and volume of healthy tissue inside the PTV, $MRgRT_{15min}$ performed better than LoP and $MRgRT_{30min}$ for whole bladder treatments. A 15 min daily adaptive radiotherapy workflow is needed to potentially benefit from replanning compared to LoP.

1. Introduction

Patients with muscle invasive bladder cancer typically have a five-year survival prognosis of about 50% [1]. Cystectomy has been the golden standard of treatment, but bladder sparing treatments involving radiotherapy have shown similar outcomes [1]. Bladder sparing treatments have the advantage of lower complication rates and improved quality of life by preserving normal bladder and sexual functions.

The wide variations in bladder size, shape and position have traditionally made it a challenging site for radiotherapy [2]. A commonly used bladder treatment strategy is the Library of Plans (LoP) strategy. Here, a "library" of planning target volumes (PTVs) and corresponding treatment plans is generated prior to treatment and the best fitting PTV is selected daily, typically based on an onboard conebeam CT (CBCT) [3–12]. For this approach it was shown that irradiated normal tissue volume and treatment margins could be reduced.

Another recent development in the field is the clinical availability of daily adaptive radiotherapy systems, CBCT-guided [13,14] as well as MR-guided systems [15–18]. These have already been shown suitable to deal with interfraction changes through daily adaptation of the treatment plan for several treatment sites and are therefore promising for bladder treatments. Vestergaard et al. have illustrated that MR-guided radiotherapy (MRgRT) has the potential to reduce irradiated normal tissue volume for bladder treatment [19] and both CBCT-guided [14] and MRgRT [20] have recently been demonstrated to be a feasible treatment modality for this tumor site. However, these studies were

* Corresponding author at: Department of Radiotherapy, Amsterdam University Medical Centers, De Boelelaan 1118, 1081 HV Amsterdam, the Netherlands.
E-mail address: d.denboer@amsterdamumc.nl (D. den Boer).
[1] Radiotherapiegroep, Nico Bolkesteinlaan 85, 7416 SE Deventer, the Netherlands.

https://doi.org/10.1016/j.phro.2021.11.002
Received 25 March 2021; Received in revised form 10 November 2021; Accepted 10 November 2021

done with a low number of bladder patients (three [14] and five [20]) and results were not compared to the current clinical practice, i.e. LoP.

Both strategies, LoP and daily adaptive radiotherapy, have their own advantages and disadvantages. A disadvantage of LoP is the chance that none of the PTVs generated prior to treatment is suitable for a specific daily situation. For daily adaptive RT the PTV is generated from the bladder of the day and the daily shape and volume can be taken into account. However, the treatment time with the presently available MRgRT systems from imaging to end of treatment delivery is typically a factor of two to three longer than the treatment time for a CBCT-based LoP strategy [5,16,20,21]. Consequently, relatively large PTV margins are needed to take into account the intrafraction filling of the bladder. Current margins reported for intrafraction changes of the bladder are typically for shorter time intervals (8–18 min) [8,11,18,21]. To speed up the daily MRgRT workflow technical developments are expected in the near future. Examples of these developments include faster auto-contouring [22] and Artificial Intelligence-assisted treatment planning reoptimization [23]. For daily adaptive CBCT-guided radiotherapy systems, times of 18 min from acceptance of first CBCT to start of irradiation have been reported for tumor sites in the pelvic region [14].

An advantage of MRgRT is the potential improvement of visualization of the soft tissues which can be taken into account with daily replanning to reduce the dose to the organs at risk (OAR). The possibility of intrafraction target monitoring and gating is also a reason to apply MRgRT [24].

The purpose of this study was to compare LoP with two daily adaptive MRgRT workflows with a total treatment time of 15 and 30 min per fraction, using clinically obtained MRgRT data. A retrospective analysis was performed to validate which strategy performs better in sparing healthy tissue and achieving target coverage. While our work focused on MRgRT, the conclusions are also relevant for CBCT-guided daily online adaptive radiotherapy.

2. Methods and materials

2.1. Patients

For the retrospective simulation, data from twenty-five lymph node metastases patients treated on a 1.5 T MR-linac (Unity, Elekta AB, Stockholm, Sweden) were used. This unique cohort was selected since bladder patients had not yet been treated with MRgRT in our institute. The included patients received clinical treatment with five fractions between August 2018 and August 2019. They provided written informed consent for use of their data as part of an ethics review board approved observational study. No specific drinking instructions were provided.

2.2. Imaging data and delineation

For each patient a pre-treatment planning CT ($0.9 \times 0.9 \times 2.0$ mm^3; Brilliance CT big bore, Philips Medical Systems, Best, NL) was used. Additionally, three MRI scans were acquired during each fraction on the MRgRT system, MRI_1, MRI_2 and MRI_3 respectively (total N = 15 for each patient) [16]. MRI image acquisition time was median two minutes. For each patient a T1 or T2 sequence was selected for the MRgRT workflow by the radiation oncologist, based on tumor visibility assessed during a pre-treatment MRI session on a 1.5 T Philips Ingenia MRI scanner (Philips Medical Systems, Best, NL). For 19/25 treatments a 3D T1-weighted scan (reconstructed voxel size $0.8 \times 0.8 \times 1.0$ mm^3; FOV $400 \times 400 \times 300$ mm^3) was selected and for 6/25 treatments a 3D T2-weighted scan (reconstructed voxel size $0.6 \times 0.6 \times 2.0$ mm^3; FOV $400 \times 400 \times 300$ mm^3). The geometrical inaccuracy in and closely around the bladder is expected to be <0.7 mm for a 1.5 T MR-linac system [25]. Bladders were manually and retrospectively delineated on all CT and MRI images leading to $Bladder_{CT}$, $Bladder_1$, $Bladder_2$ and $Bladder_3$.

2.3. Clinical MRgRT workflow

For each treatment fraction of the patient group mentioned above, daily online replanning was performed following the Adapt to Shape workflow of the Elekta Unity as described previously by Werensteijn-Honingh et al. [16]. Each fraction, contours from the pre-treatment planning CT were propagated on the daily MRI using rigid and deformable registration.

Electron density was based on assignment to structures. If necessary, contours of GTV and OARs were manually adapted. The treatment plan, consisting of seven IMRT beams, was reoptimized for each fraction. A secondary dose calculation was performed with a separate treatment planning system, Oncentra version 4.5.2 (Elekta AB, Stockholm, Sweden). Irradiation was done with 7MV FFF. In the manuscript we will refer to this workflow as the "current" MRgRT workflow, illustrating the current capabilities of the MRgRT commercial system. The steps in this workflow are expected to take the same time for this patient group as for bladder patients [17,18]. As only a small part of the time is spent on irradiation [16], this time is not expected to change drastically when a different dose per fraction is given.

2.4. Simulated MRgRT approach

Two MRgRT daily optimization strategies were simulated: 1) a workflow based on the median time between MRI_1 and MRI_3 of 30 min (range 21–57 min), $MRgRT_{30min}$, illustrating the current capabilities of an MRgRT commercial system and 2) a workflow, based on the median time between MRI_1 and MRI_2 of 15 min (range 8–25 min), $MRgRT_{15min}$, illustrating a hypothetical optimized workflow (Fig. 1). For $MRgRT_{15min}$ all online adaptive steps including radiation delivery were assumed between MRI_1 and MRI_2 and for $MRgRT_{30min}$ these steps were between MRI_1 and MRI_3 (with the online adaptive steps between MRI_1 and MRI_2 and radiation delivery between MRI_2 and MRI_3 [16]).

PTVs were constructed from $Bladder_1$ on MRI_1 by population-based margins for $MRgRT_{15min}$ and $MRgRT_{30min}$. Published data on margins are typically not validated for 30 min, but for shorter time intervals [8,11,19,26]. Therefore the margins to account for the intra-fraction bladder changes (intra-fraction patient motion, centroid motion and bladder filling) were constructed from the MRgRT dataset. To determine appropriate margins the delineated bladders on the MRI_1 were asymmetrically expanded in six directions (left, right, anterior, posterior, inferior and superior) in steps of 1 mm until the delineated bladder on the MRI_3 or MRI_2 scan was completely encompassed for $MRgRT_{30min}$ and $MRgRT_{15min}$ strategy, respectively. Ten of the twenty-five patients were randomly selected. Population-based PTV margins were derived from these ten patients (N = 50 fractions). Margins were constructed for each direction by placing a 90% inclusion criterion on individual treatment fractions. The most commonly used margin recipe [27] uses 90% of patients instead of fractions, but in our case a new treatment plan would be generated for each fraction. This random selection and subsequent margin calculation was done to minimize bias and repeated 1000 times. Finally, the mean values were used for the analysis in this manuscript (see Supplementary Material A for more details).

2.5. Simulated LoP approach

The bladder was contoured on the planning CT and expanded to create two PTVs to fill the library. The expansion for PTV LoP Tight was 6/6 mm left/right, 10/10 mm ant/post and 6/10 mm inf/sup and for PTV LoP Wide: 10/10 mm left/right, 15/15 mm ant/post and 10/15 mm inf/sup. These values were based on literature [3,10] and clinical practice in our institute for CBCT-guided radiotherapy. The methodology is a further adaptation of the work as described previously by Willems et al. [28]. Daily plan selection was based on the contoured bladder on MRI_1, the smallest LoP PTV was selected that encompassed the complete bladder, named PTV LoP Selected. If the bladder on MRI_1 did

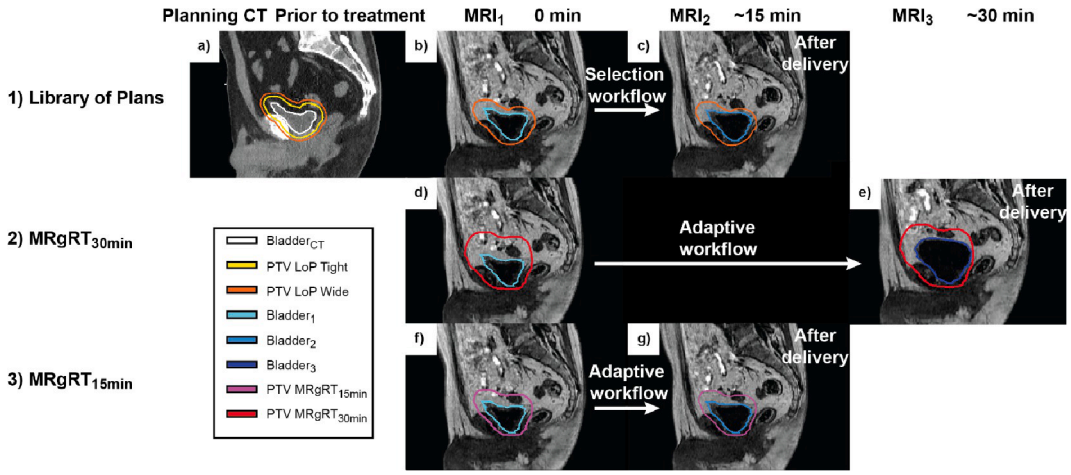

Fig. 1. Illustration of the LoP strategy and the two MRgRT strategies ($MRgRT_{30min}$ and $MRgRT_{15min}$). 1) illustrates the LoP strategy. a) The bladder was delineated on the planning CT and two PTVs were constructed (PTV LoP Tight and PTV LoP Wide). b) Based on $Bladder_1$ the most suitable PTV was selected (in this case PTV LoP Wide). c) MRI_2 was considered the simulated post-treatment image. Evaluation of PTV LoP Selected was done with $Bladder_2$. 2) illustrates the $MRgRT_{30min}$ workflow. d) A PTV was constructed from $Bladder_1$ with population-based margins. e) This PTV was evaluated with the MRI_3 as simulated post-treatment image using $Bladder_3$. 3) illustrates the $MRgRT_{15min}$ workflow. f) Similar to the $MRgRT_{30min}$, a PTV was constructed from $Bladder_1$. g) Evaluation was now done with MRI_2 as simulated post-treatment image using $Bladder_2$.

not fit completely within either of the LoP PTVs or if the bladder was too empty (if there was more than one cm distance between the bladder and the PTV in all directions except caudal), the fraction was not included in the analysis in line with clinical practice. In these cases, the patient would be asked to void the bladder or to drink additional liquid. Plan selection and radiotherapy delivery were assumed between MRI_1 and MRI_2 with a time interval of about 15 min which corresponded well to reported CBCT LoP studies with time intervals between 9 and 19 min [12,29,30].

2.6. Treatment strategy evaluation and statistics

To evaluate the efficacy of the LoP and MRgRT approaches, the volume of healthy tissue in the PTV and the relative volume of the bladder outside the PTV were analyzed on the simulated post-treatment MRI images: MRI_2 for LoP and $MRgRT_{15min}$, and MRI_3 for $MRgRT_{30min}$.

Volumes were determined with an in-house developed software package, Volumetool [31]. Fractions were only included in the statistical comparison when an LoP PTV was selected. The analysis we present was by pooling over the different scans for the patients. The differences in volumes between the strategies were tested by the two-tailed Wilcoxon matched-pairs signed-rank test; $p < 0.05$ was considered significant.

3. Results

Margins (mean ± standard deviation) for the two MRgRT strategies were 11 ± 2/17 ± 2 mm left/right, 24 ± 6/13 ± 2 mm ant/post and 36 ± 5/5 ± 1 mm sup/inf for $MRgRT_{30min}$ and 8 ± 1/10 ± 1 mm left/right, 12 ± 2/11 ± 1 mm ant/post and 18 ± 2/4 ± 1 mm sup/inf for $MRgRT_{15min}$. The margins were asymmetric with the highest values for anterior and superior directions.

For the comparison of LoP vs. MRgRT strategies 107/125 fractions were included. For 7/125 fractions the PTV LoP Wide did not completely encompass the delineated bladder on MRI_1 and for 11/125 fractions the bladder was too empty. PTV LoP Tight and Wide were selected 73 and 34 times. The median and range of the bladder volumes at CT, MRI_1, MRI_2 and MRI_3, as well as the PTVs for all three strategies are presented in Table 1. The median bladder filling speed was respectively 1.6 cm^3/min (range 0.3–12.0 cm^3/min) and 1.3 cm^3/min (range 0.1–9.3 cm^3/min) between MRI_3 and MRI_1, and MRI_2 and MRI_1.

Table 1
Median and range are shown for bladder volumes on simulated pre-treatment scan and on three time points during simulated whole bladder radiotherapy based on 125 fractions of 25 patients treated with MRgRT, as well as median and range of PTVs of the three investigated radiotherapy approaches: Library of Plans (LoP) with fraction time of 15 min, $MRgRT_{15min}$ with fraction time of 15 min and $MRgRT_{30min}$ with fraction time of 30 min.

Structure		N [–]	Volume [cm^3]
Bladder			
	Planning CT	25	97 (37–239)
	MRI_1	107[1]	83 (31–284)
		125	83 (31–593)
	MRI_2	107[1]	103 (46–411)
		125	104 (46–680)
	MRI_3	107[1]	136 (53–570)
		125	136 (53–703)
PTV			
	LoP Tight	25	245 (105–438)
	LoP Wide	25	348 (164–581)
	$LoP_{Selected}$	107[1]	270 (105–546)
	$MRgRT_{15min}$	107[1]	265 (134–620)
		125	261 (134–1127)
	$MRgRT_{30min}$	107[1]	466 (263–970)
		125	462 (263–1646)

[1] Based on 107/125 fractions for which one of the two LoP plans was adequate for the observed bladder volume and patient would not be asked to void or drink.

For the $MRgRT_{30min}$ workflow the volumes of the PTVs were up to 75% larger than for the other two strategies, with a median value of 466 cm^3 compared to 270 cm^3 for the selected LoP PTVs and 265 cm^3 for the PTVs of $MRgRT_{15min}$.

The volumes of healthy tissue inside the PTV and target outside the PTV on the simulated post-treatment image are presented in Table 2. The median volume of healthy tissue inside the PTV was 332 cm^3 for $MRgRT_{30min}$ and corresponded to 71% of the PTV. This volume was significantly larger ($p < 0.01$) than for $MRgRT_{15min}$ and LoP with values of 151 and 150 cm^3 respectively (Fig. 2a). For $MRgRT_{15min}$ and LoP the volumes of healthy tissue inside the PTV did not significantly differ, $p = 0.11$.

The median value of target volume, i.e. bladder volume, outside the PTV on the simulated post-treatment image was 0.0 cm^3 for all three methods (Fig. 2b). The $MRgRT_{15min}$ strategy did not perform significantly better than the $MRgRT_{30min}$ strategy, $p = 0.39$, however both

Table 2
Median and range of volumes for healthy tissue inside PTV and missed target on simulated post-treatment images for whole bladder radiotherapy simulated with 125 fractions of 25 patients treated with MRgRT. Volumes are shown for three radiotherapy approaches: Library of Plans (LoP) with fraction time of 15 min, $MRgRT_{15min}$ with fraction time of 15 min and $MRgRT_{30min}$ with fraction time of 30 min.

Method	N [–]	Healthy tissue in PTV [cm^3]	Missed target [cm^3]	Missed target [%]
LoP				
	107[1]	150 (28–299)	0 (0–48)	0 (0–23)
$MRgRT_{15min}$				
	107[1]	151 (59–260)	0 (0–28)	0 (0–10)
	125	151 (59–447)	0 (0–28)	0 (0–10)
$MRgRT_{30min}$				
	107[1]	332 (136–537)	0 (0–100)	0 (0–20)
	125	315 (135–941)	0 (0–100)	0 (0–20)

[1] Based on 107/125 fractions for which one of the two LoP plans was adequate for the observed bladder volume and patient would not be asked to void or drink.

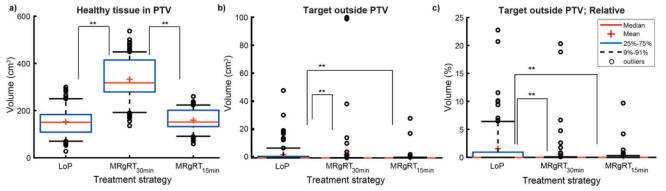

Fig. 2. Simulated volume of healthy tissue inside PTV and missed target volume in post-treatment image (MRI_2 for LoP and $MRgRT_{15min}$, MRI_3 for $MRgRT_{30min}$) for whole bladder treatment using three treatment strategies $MRgRT_{30min}$, $MRgRT_{15min}$ and LoP based on 25 treatments of 5 fractions. Data shown for 107 fractions (18 were excluded due to too full or too empty bladder filling for LoP). ** indicates significance of $p < 0.01$, by two-tailed Wilcoxon matched-pairs signed-rank test a) The volume of healthy tissue inside the PTV in the post-treatment image. b) The volume of bladder outside the PTV in the post-treatment image. c) Relative volumes of the bladder (in %) outside the PTV in the post-treatment image.

performed better than the LoP strategy, $p < 0.01$ (Fig. 2b). The relative volume of bladder outside the PTV on the post-treatment MRI was lower for $MRgRT_{15min}$ than for LoP. The 75%–91% whisker in the boxplot, corresponding to 19 fractions was between 0.5 and 6.5% for LoP and 0.0–0.3% for $MRgRT_{15min}$ (Fig. 2c). The LoP strategy also showed outliers up to 21–23% of missed target volume, whereas the highest value for $MRgRT_{15min}$ was 10%. Some practical examples of bladder outside the PTV (missed target) are given in Fig. 3, where 17–28 cm^3 and 100 cm^3 of the target (bladder) were missed.

4. Discussion

To the best of our knowledge, this is the first study comparing LoP with MRgRT for whole bladder treatments using clinical MRgRT data. Two daily adaptive MRgRT strategies with a median time of 15 min, $MRgRT_{15min}$, and 30 min, $MRgRT_{30min}$, between first image and end of treatment were compared to our clinically used LoP strategy. The $MRgRT_{30min}$ workflow had more healthy tissue inside the PTV than the LoP strategy. The $MRgRT_{15min}$ workflow had a similar volume of healthy tissue inside the PTV as LoP and missed less target.

Limitations of our study were the use of data of patients that did not have bladder cancer and the absence of a drinking protocol. The filling can be described as a "comfortably filled bladder". However, the observed starting bladder volumes (median 97 cm^3 at start of treatment) corresponded well with reported valued of bladder patients with drinking protocols, with a range of 100–130 cm^3 [6,7,11,19,32]. The bladder filling speed of median 1.6 cm^3/min between MRI_1 and MRI_3 and 1.3 cm^3/min between MRI_1 and MRI_2 were also in the range of reported values ranging from 0.8 to 2.1 cm^3/min [26,32–35]. Even with a drinking protocol, large interpatient and interfraction variations typically still occur [33,34]. It has been shown that for empty and full bladder, the same values could be used in terms of margins [26,36].

The PTV margins found in this study for $MRgRT_{15min}$ strategy corresponded very well to margins reported in literature for studies with similar intrafraction time intervals [8,11,19,32], with values of 5–10/5–10 mm left/right, 8–14/9–14 mm ant/post and 13–33/5–6 mm sup/inf. The $MRgRT_{15min}$ margins fit well within the clinically used expansions for generating the LoP PTVs.

The PTV margins determined for the $MRgRT_{30min}$ workflow were relatively large, compared to other publications [6,8,11,19,20,26,36]. This was mostly due to the relatively long treatment time in comparison to the investigated time frames in other studies (8–18 min). In the study of Hunt et al. [20], the PTV margins (5/5 mm left/right, 15/10 mm ant/post and 15/5 mm sup/inf) covered 90% of the bladder at the 30 min time point, instead of the 100% for $MRgRT_{30min}$ in our study. The

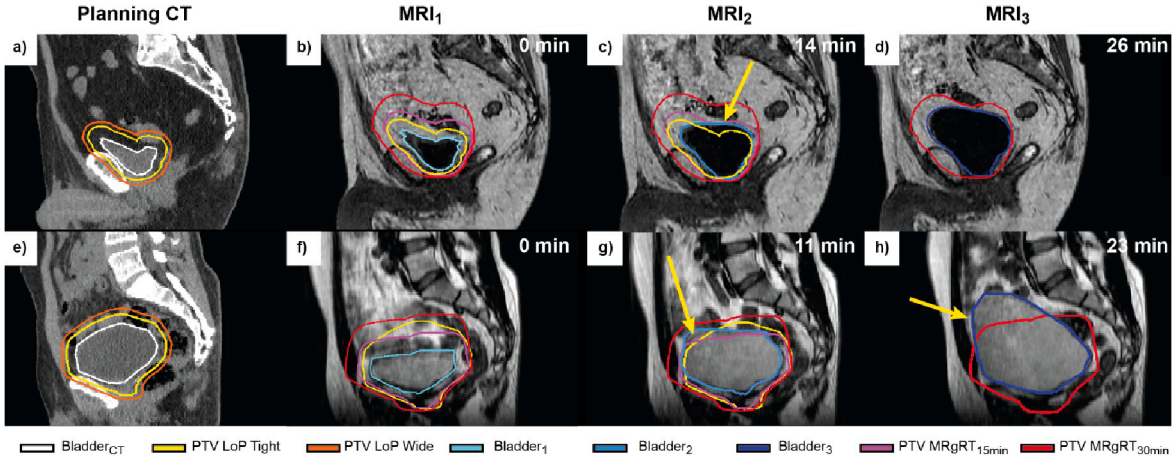

Fig. 3. Two examples shown in the sagittal plane, illustrating exceptions; one or more of the strategies led to part of the bladder being outside the PTV in the simulated post-treatment image. Time of the image indicated in top right corner. a–d) Example 1. Planning CT (a) and T1 weighted images (b–d). The selected LoP PTV (yellow) was sufficient in MRI_1, but missed a part (29 cm^3) of the bladder in MRI_2 (indicated by the yellow arrow in c). (e–h) Example 2. Planning CT (a) and T2 weighted images (f–h). The PTVs of all three strategies missed a part of the bladder in the simulated post-treatment MRI. For LoP and $MRgRT_{15min}$: 17 cm^3 and 28 cm^3 of the $Bladder_2$ was outside the PTV respectively (indicated by the yellow arrow in g). For the $MRgRT_{30min}$ workflow: 100 cm^3 of the $Bladder_3$ was outside the PTV (indicated by the yellow arrow in h).

median intrafraction filling volume of the five patients studied in Hunt et al. [20], including one with a catheter, was 30 cm^3 compared to 48 cm^3 in our study.

The PTV margins of the MRgRT workflows were constructed from the same dataset as used for the comparison with LoP, this is a limitation of our study and could introduce bias for $MRgRT_{30min}$ and $MRgRT_{15min}$. To mitigate this, margin construction was done with a repeated randomly selected subset of the patients and using the obtained mean values.

The advantage of the daily reoptimization using the $MRgRT_{30min}$ workflow compared to the LoP strategy was canceled out due to the needed relatively large population-based margins. The use of patient-specific margins could lead to a reduction in PTV volume and radiation exposure to healthy tissue. Published work showed promising results in this direction [8,37].

For the LoP strategy, fractions were excluded following the clinical workflow, when the patients bladder was too full or too empty and no appropriate LoP PTV was available. This occurred in 14% (18/125) of the treatment fractions. This shows an advantage of the MRgRT strategies, where the treatment would have continued, as there is no dependency on a predefined library. While this approach is in line with the clinical workflow, the fact that these fractions were excluded from the analysis could potentially introduce a bias for the LoP workflow.

The differences between the LoP and $MRgRT_{15min}$ strategies in terms of target coverage and normal tissue in the PTV were small and bladder patients can be treated adequately with a CBCT-guided LoP strategy. However there are other advantages for using MRgRT. With the soft tissue contrast combined with daily adaptive radiotherapy, it has the potential to decrease toxicity of surrounding OARs [38]. In addition, the soft tissue contrast can visualize the tumor and allow a boost of this area without the need for implanted markers (which would be the case for CBCT-guided RT). MRgRT also allows for intrafraction monitoring and gating.

In conclusion, $MRgRT_{15min}$ performed best, closely followed by LoP and then $MRgRT_{30min}$ for whole bladder treatments, taking into account the target coverage and the amount of healthy tissue inside the PTV. To be able to use MRgRT for whole bladder treatments including its functionalities, it is necessary to further optimize and accelerate the MRgRT workflow.

Conflict of Interest Notification

The overarching University Medical Center Utrecht MR-linac scientific project, including employment of one of the authors, has been partly funded by Elekta AB (Stockholm, Sweden). Elekta did not have any part in the design, execution or analysis of this study. The authors declared that there is no other conflict of interest.

Funding

None.

Declaration of Competing Interest

The authors declare that they have no known competing financial interests or personal relationships that could have appeared to influence the work reported in this paper.

Acknowledgements

The authors want to acknowledge Simon Woodings for providing language help during the preparation of this manuscript.

Appendix A. Supplementary data

Supplementary data to this article can be found online at https://doi.org/10.1016/j.phro.2021.11.002.

References

[1] Arcangeli G, Arcangeli S, Strigari L. A systematic review and meta-analysis of clinical trials of bladder-sparing trimodality treatment for muscle-invasive bladder cancer (MIBC). Crit Rev Oncol Hematol 2015;94:105–15. https://doi.org/10.1016/j.critrevonc.2014.11.007.

[2] Turner SL, Swindell R, Bowl N, Marrs J, Brookes B, Read G, et al. Bladder movement during radiation therapy for bladder cancer: implications for treatment planning. Int J Radiat Oncol Biol Phys 1997;39:355–60. https://doi.org/10.1016/S0360-3016(97)00070-9.

[3] Lalondrelle S, Huddart R, Warren-Oseni K, Hansen VN, McNair H, Thomas K, et al. Adaptive-Predictive Organ Localization Using Cone-Beam Computed Tomography for Improved Accuracy in External Beam Radiotherapy for Bladder Cancer. Int J Radiat Oncol Biol Phys 2011;79:705–12. https://doi.org/10.1016/j.ijrobp.2009.12.003.

[4] Foroudi F, Wong J, Kron T, Rolfo A, Haworth A, Roxby P, et al. Online adaptive radiotherapy for muscle-invasive bladder cancer: results of a pilot study. Int J Radiat Oncol Biol Phys 2011;81(3):765–71. https://doi.org/10.1016/j.ijrobp.2010.06.061.

[5] Meijer GJ, van der Toorn PP, Bal M, Schuring D, Weterings J, de Wildt M. High precision bladder cancer irradiation by integrating a library planning procedure of 6 prospectively generated SIB IMRT plans with image guidance using lipiodol markers. Radiother Oncol 2012;105:174–9. https://doi.org/10.1016/j.radonc.2012.08.011.

[6] McDonald F, Lalondrelle S, Taylor H, Warren-Oseni K, Khoo V, McNair HA, et al. Clinical Implementation of Adaptive Hypofractionated Bladder Radiotherapy for Improvement in Normal Tissue Irradiation. Clin Oncol (R Coll Radiol) 2013;25:549–56. https://doi.org/10.1016/j.clon.2013.06.001.

[7] Vestergaard A, Kallehauge JF, Petersen JBB, Høyer M, Søndergaard J, Muren LP. An adaptive radiotherapy planning strategy for bladder cancer using deformation vector fields. Radiother Oncol 2014;112:371–5. https://doi.org/10.1016/j.radonc.2014.07.012.

[8] Grønborg C, Vestergaard A, Høyer M, Söhn M, Pedersen EM, Petersen JB, et al. Intra-fractional bladder motion and margins in adaptive radiotherapy for urinary bladder cancer. Acta Oncol 2015;54:1461–6. https://doi.org/10.3109/0284186X.2015.1062138.

[9] Lutkenhaus LJ, Visser J, de Jong R, Hulshof MCCM, Bel A. Evaluation of delivered dose for a clinical daily adaptive plan selection strategy for bladder cancer radiotherapy. Radiother Oncol 2015;116:51–6.

[10] Murthy V, Masodkar R, Kalyani N, Mahantshetty U, Bakshi G, Prakash G, et al. Clinical Outcomes With Dose-Escalated Adaptive Radiation Therapy for Urinary Bladder Cancer: A Prospective Study. Int J Radiat Oncol Biol Phys 2016;94:60–6. https://doi.org/10.1016/j.ijrobp.2015.09.010.

[11] Foroudi F, Pham D, Bressel M, Gill S, Kron T. Intrafraction bladder motion in radiation therapy estimated from pretreatment and posttreatment volumetric imaging. Int J Radiat Oncol Biol Phys 2013;86:77–82. https://doi.org/10.1016/j.ijrobp.2012.11.035.

[12] Collins SD, Leech MM. A review of plan library approaches in adaptive radiotherapy of bladder cancer. Acta Oncol 2018;57:566–73. https://doi.org/10.1080/0284186X.2017.1420908.

[13] Archambault Y, Boylan C, Bullock D, Morgas T, Peltola J, Ruokokoski E, et al. Making on-Line Adaptive Radiotherapy Possible Using Artificial Intelligence and Machine Learning for Efficient Daily Re-Planning. Med Phys Int 2020;8:77–86.

[14] Sibolt P, Andersson LM, Calmels L, Sjöström D, Bjelkengren U, Geertsen P, et al. Clinical implementation of artificial intelligence-driven conebeam computed tomography-guided online adaptive radiotherapy in the pelvic region. Phys Imaging Radiat Oncol 2021;17:1–7. https://doi.org/10.1016/j.phro.2020.12.004.

[15] Henke LE, Contreras JA, Green OL, Cai B, Kim H, Roach MC, et al. Magnetic Resonance Image-Guided Radiotherapy (MRIgRT) A 4.5-Year Clinical Experience. Clin Oncol (R Coll Radiol) 2018;30:720–7. https://doi.org/10.1016/j.clon.2018.08.010.

[16] Werensteijn-Honingh AM, Kroon PS, Winkel D, Aalbers EM, van Asselen B, Bol GH, et al. Feasibility of stereotactic radiotherapy using a 1.5 T MR-linac: Multi-fraction treatment of pelvic lymph node oligometastases. Radiother Oncol 2019;134:50–4. https://doi.org/10.1016/j.radonc.2019.01.024.

[17] de Muinck Keizer DM, Kerkmeijer LGW, Willigenburg T, van Lier ALHMW, Hartogh MDD, van der Voort van Zyp JRN, et al. Prostate intrafraction motion during the preparation and delivery of MR-guided radiotherapy sessions on a 1.5T MR-Linac. Radiother Oncol 2020;151:88–94. https://doi.org/10.1016/j.radonc.2020.06.044.

[18] Tetar SU, Bruynzeel AME, Lagerwaard FJ, Slotman BJ, Bohoudi O, Palacios MA. Clinical implementation of magnetic resonance imaging guided adaptive radiotherapy for localized prostate cancer. Phys Imaging Radiat Oncol 2019;9:69–76. https://doi.org/10.1016/j.phro.2019.02.002.

[19] Vestergaard A, Hafeez S, Muren LP, Nill S, Høyer M, Hansen VN, et al. The potential of MRI-guided online adaptive re-optimisation in radiotherapy of urinary bladder cancer. Radiother Oncol 2016;118:154–9. https://doi.org/10.1016/j.radonc.2015.11.003.

[20] Hunt A, Hanson I, Dunlop A, Barnes H, Bower L, Chick J, et al. Feasibility of Magnetic Resonance Guided Radiotherapy for the Treatment of Bladder Cancer. Clin Transl Radiat Oncol 2020;25:46–51. https://doi.org/10.1016/j.ctro.2020.09.002.

[21] Hafeez S, Warren-Oseni K, McNair HA, Hansen VN, Jones K, Tan M, et al. Prospective study delivering simultaneous integrated highdose tumor boost (≤ 70 Gy) with image guided adaptive radiation therapy for radical treatment of localized muscle-invasive bladder cancer. Int J Radiat Oncol Biol Phys 2016;94:1022–30. https://doi.org/10.1016/j.ijrobp.2015.12.379.
[22] Sharp G, Fritscher KD, Pekar V, Peroni M, Shusharina N, Veeraraghavan H, et al. Vision 20/20: perspectives on automated image segmentation for radiotherapy. Med Phys 2014;41:050902. https://doi.org/10.1118/1.4871620.
[23] Kontaxis C, Bol GH, Lagendijk JJW, Raaymakers BW. DeepDose: Towards a fast dose calculation engine for radiation therapy using deep learning. Phys Med Biol 2020;65:075013. https://doi.org/10.1088/1361-6560/ab7630.
[24] Mutic S, Dempsey JF. The ViewRay system: Magnetic Resonance-Guided and controlled radiotherapy. Semin Radiat Oncol 2014;24:196–9. https://doi.org/10.1016/j.semradonc.2014.02.008.
[25] Tijssen RHN, Philippens MEP, Paulson ES, Glitzner M, Chugh B, Wetscherek A, et al. MRI commissioning of 1.5T MR-linac systems – a multi-institutional study. Radiother Oncol 2019;132:114–20. https://doi.org/10.1016/j.radonc.2018.12.011.
[26] Dees-Ribbers HM, Betgen A, Pos FJ, Witteveen T, Remeijer P, van Herk M. Inter- and intra-fractional bladder motion during radiotherapy for bladder cancer: A comparison of full and empty bladders. Radiother Oncol 2014;113:254–9. https://doi.org/10.1016/j.radonc.2014.08.019.
[27] Van Herk M. Errors and margins in radiotherapy. Semin Radiat Oncol 2004;14:52–64. https://doi.org/10.1053/j.semradonc.2003.10.003.
[28] Willems NJW, Kroon PS, Boer JCJ, Meijer GJ, Zyp JRN, Noteboom JL. EP-1844: Clinical introduction of simple adaptive radiotherapy for transitional cell bladder carcinoma. Radiother Oncol 2017;05:S1009. https://doi.org/10.1016/S0167-8140(17)32279-X.
[29] Adil K, Popovic M, Cury FL, Faria SL, Duclos M, Souhami L. Anisotropic bladder planning target volume in bladder radiation therapy. Pract Radiat Oncol 2019;9:24–8. https://doi.org/10.1016/j.prro.2018.07.006.
[30] Krishnan A, Tsang YM, Stewart-Lord A. The impact of intra-fractional bladder filling on "Plan of the day" adaptive bladder radiotherapy. Tech Innov Patient Support Radiat Oncol 2019;9:31–4. https://doi.org/10.1016/j.tipsro.2019.01.001.
[31] Bol GH, Kotte ANTJ, van der Heide UA, Lagendijk JJW. Simultaneous multi-modality ROI delineation in clinical practice. Comput Methods Programs Biomed 2009;96:133–40. https://doi.org/10.1016/j.cmpb.2009.04.008.
[32] Mangar SA, Scurr E, Huddart RA, Sohaib SA, Horwich A, Dearnaley DP, et al. Assessing intra-fractional bladder motion using cine-MRI as initial methodology for Predictive Organ Localization (POLO) in radiotherapy for bladder cancer. Radiother Oncol 2007;85:207–14. https://doi.org/10.1016/j.radonc.2007.04.037.
[33] McBain CA, Khoo VS, Buckley DL, Sykes JS, Green MM, Cowan RA, et al. Assessment of bladder motion for clinical radiotherapy practice using cine-magnetic resonance imaging. Int J Radiat Oncol Biol Phys 2009;75:664–71. https://doi.org/10.1016/j.ijrobp.2008.11.040.
[34] Søndergaard J, Olsen KO, Muren LP, Elstrøm UV, Grau C, Høyer M. A study of image-guided radiotherapy of bladder cancer based on lipiodol injection in the bladder wall. Acta Oncol 2010;49:1109–15. https://doi.org/10.3109/02841861003789491.
[35] McBain CA, Green MM, Stratford J, Davies J, McCarthy C, Taylor B, et al. Ultrasound imaging to assess inter- and intra-fraction motion during bladder radiotherapy and its potential as a verification tool. Clin Oncol (R Coll Radiol) 2009;21:385–93. https://doi.org/10.1016/j.clon.2009.01.016.
[36] Wilson C, Moseshvili E, Tacey M, Quin I, Lawrentschuk N, Bolton D, et al. Assessment of intrafraction motion of the urinary bladder using magnetic resonance imaging (cineMRI). Clin Oncol (R Coll Radiol) 2020;32:101–9. https://doi.org/10.1016/j.clon.2019.09.056.
[37] Krywonos J, Fenwick J, Elkut F, Jenkinson I, Liu YH, Brunt JNH, et al. MRI image-based FE modelling of the pelvis system and bladder filling. Comput Methods Biomech Biomed Engin 2010;13:669–76. https://doi.org/10.1080/10255840903446961.
[38] Winkel D, Kroon PS, Werensteijn-Honingh AM, Bol GH, Raaymakers BW, Jürgenliemk-Schulz IM. Simulated dosimetric impact of online replanning for stereotactic body radiation therapy of lymph node oligometastases on the 1.5T MR-linac. Acta Oncol 2018;57:1705–12. https://doi.org/10.1080/0284186X.2018.1512152.